

RESEARCH

Open Access



A practical hybrid approach to the problem of surveying a working historical bell considering innovative measurement methods

Izabela Skrzypczak¹ , Grzegorz Oleniacz¹ , Agnieszka Leśniak^{2*} , Maria Mrówczyńska³ ,
Marta Rymar⁴ and Mariusz Oleksy⁵

Abstract

The article proposes using a novel hybrid measurement method, with expected precision results, to determine the characteristic of the historic, 17th-century bell. In an interdisciplinary approach, modern and non-invasive physical and chemical measurement methods were used. Based on the monitoring (measurements and laser scanning), a three-dimensional geometric model was built to calculate the bell size and analyze its condition depending on material consumption. Next, chemical measures of the bell samples were carried out to determine the material properties. For that purpose, advanced precision microscopic techniques were used. Based on the geometric model and chemical studies, the material properties and density of the bronze were determined using additive assumptions. Measurement accuracy and data quality were evaluated statistically. The method allows reliably determining the bell's weight without needing to dismantle it or external intervention. The approach is helpful for practitioners performing conservation work on such objects.

Keywords Historical bell, Non-contact measurements, Laser scanning, Chemical microstructure studies, Material properties, 3D model

Introduction

Church bells, from the point of view of their function, are musical instruments that belong the group of idiophones. Their sound is generated by vibrations of the bell caused by repeated striking of the clapper. In the European tradition, this is most often achieved by swinging

the entire bell, which results in significant inertial forces transferred to the supporting structure. Structural and material problems related to the design and use of bells are researched by modelling the behaviour of the bell and the dynamics of the belfry while the bell is striking [1, 2], and by analysing forces transferred to the belfry structure [3, 4]. For this reason, the impact of the swinging of the bell is important when checking the ultimate limit state of the structure of the entire building (belfry) [5–8]. The effect of bell-ringing on bell-towers was described in [9]. The paper [10] discusses a bell tower's structure reaction under service loads arising during use. In [11], dynamic experimental tests were used to detect excessive movements on the tower when the bell's moving.

Assessment of the technical condition of structures, including historical structures such as belfries, should comprise geodetic monitoring [12, 13], in particular, measurements of displacements and deformations, which

*Correspondence:

Agnieszka Leśniak
agnieszka.lesniak@pk.edu.pl

¹ Faculty of Civil, Environmental Engineering and Architecture, Rzeszow University of Technology, al. Powstańców Warszawy 12, 35-959 Rzeszów, Poland

² Faculty of Civil Engineering, Cracow University of Technology, ul. Warszawska 24, 31-155 Kraków, Poland

³ Institute of Civil Engineering, University of Zielona Góra, ul. Prof. Z. Szafrana 1, 65-516 Zielona Góra, Poland

⁴ Craft Museum in Krosno, ul. Piłsudskiego 19, 38-400 Krosno, Poland

⁵ Faculty of Chemistry, Rzeszow University of Technology, al. Powstańców Warszawy 12, 35-959 Rzeszów, Poland



© The Author(s) 2023. **Open Access** This article is licensed under a Creative Commons Attribution 4.0 International License, which permits use, sharing, adaptation, distribution and reproduction in any medium or format, as long as you give appropriate credit to the original author(s) and the source, provide a link to the Creative Commons licence, and indicate if changes were made. The images or other third party material in this article are included in the article's Creative Commons licence, unless indicated otherwise in a credit line to the material. If material is not included in the article's Creative Commons licence and your intended use is not permitted by statutory regulation or exceeds the permitted use, you will need to obtain permission directly from the copyright holder. To view a copy of this licence, visit <http://creativecommons.org/licenses/by/4.0/>. The Creative Commons Public Domain Dedication waiver (<http://creativecommons.org/publicdomain/zero/1.0/>) applies to the data made available in this article, unless otherwise stated in a credit line to the data.

are the first and basic symptom of unfavourable phenomena occurring in historical buildings. Geodetic monitoring is planned and conducted in a way that depends on the structure of the object, its location, the speed and size of the occurring deformations and the geodetic technology used [14, 15]. Monitoring also involves the need to perform periodically repeated measurements aimed at identifying changes in objects over time [16]. When geodetic methods are used, displacements are very often determined through a series of measurements carried out in a network of measurement and control points with an optimized structure set up on the object [17]. Modern measurement technologies enable geodetic monitoring of historical objects using classic geodetic methods [18], gravimetric measurements, the GNSS system [19], unmanned aerial vehicles, laser scanning [20], GIS technology and artificial intelligence [21, 22]. Displacements and deformations of elements of historical engineering structures can be determined using modern measuring instruments (laser total stations, laser measuring stations). These are classic measurement methods, which enable high precision distance measurements, reaching $\pm 15 \mu\text{m} + 6 \mu\text{m/m}$ when the distance is measured with a prism with an operational range of 120 m [23].

Laser scanning technology has been used for obtaining data and performing measurements to obtain the digital form of objects. It is one of the fastest and most economical methods for identifying the geometry of objects [24–26]. The importance of laser scanning has been confirmed by many researchers, and the areas of application in scientific research and engineering are very wide, including: mining [27], geology [28], topography [29], archaeology [30], civil engineering and architecture [31–33]. The use of 3D laser scanning technology to measure a building makes it possible to obtain a point cloud and produce digital documentation to create a BIM (Building Information Modelling) model of the object scanned. Nevertheless, it should be emphasized that TLS (Terrestrial Laser Scanning) and photogrammetric measurements have been used for visualization and modelling of steel structures [34], inventory of complex industrial, residential and historic buildings [35], monitoring the condition of structures, measuring displacements and strains [36, 37], and automatic classification of building materials [38]. TLS measurements are currently widely used for inventory work, also for modelling information about monuments or historical buildings—Historical Building Information Modelling (HBIM) [39–44]. This technology makes it possible to prepare precise architectural documentation including: projections, sections, elevations, 3D models or multimedia visualizations [45–47].

In HBIM it is not only important to build a model of the object, but also to obtain data about the characteristics of

the material from which the object was made. In order to determine the characteristic structure and elemental composition of materials, microscopic techniques are most often used. They guarantee high precision and accuracy, and provide results very fast [48, 49]. The use of various microscopic techniques in historical, conservation [50–52] and archaeological research [53], including the study of monuments/artefacts [54–56] and materials [57–62], is aimed at obtaining enlarged images of small objects, their details and properties. In this way, various information is obtained on a microscopic scale, e.g. about the shape, size, structure or morphology and topography of the objects examined. In terms of the type of radiation and imaging methods, microscopes used for specialist examination of artefacts can be divided into two basic types: optical microscopes and electron microscopes [50, 53]. Optical microscopes are basic laboratory instruments that enable efficient observation and identification of the structure of objects/samples and performance of necessary micro measurements. Electron microscopes use an electron beam for imaging and provide accurate images of the surface microstructure of various small objects.

Scanning electron microscopy (SEM), on the other hand, is complementary to optical microscopy and enables more accurate imaging of the surface microstructures of various objects of much smaller size. This measurement technique consists in scanning the surface of a sample with an electron beam shaped by the microscope system. SEM can also be used to perform, quantitative point analyses of the chemical composition of samples. The Energy Dispersive X-ray Spectroscopy (EDS) technique is most often used for spot determination of the chemical composition of artefacts because quantitative results of analyses can be obtained from a particular point in a matter of seconds. Another type of optical research technology is glow discharge spectroscopy, which enables direct analysis of solid samples. Glow discharge spectrometers were first used mainly in the steel industry to examine galvanized sheets and passivation films on steel surfaces [51]. At present, it is one of the most favourable techniques used for surface analysis, i.e. for profiling the surface and depth of materials [53]. Since the use of modern microscopic techniques guarantees accurate measurements, and results are obtained immediately, these techniques were used for part of the research.

Since there is a need to analyse the structure of the church belfry in terms of statics and dynamics, and also because of arguments among local historians and ethnographers [63], research was undertaken to accurately determine the actual mass of the bell. The article proposes a methodology based on geodetic measurements of

the geometry of the bell to indirectly determine its mass and the shape (external and internal surfaces), thus enabling the calculation of its volume. The measurements of the chemical structure of the bell carried out in the next stage consisted in analysing its chemical composition using modern microscopic EDS techniques. The subject of the research presented in this paper is the bell "Urban".

The authors were an interdisciplinary research team that consisted of construction engineers, geodesists, chemists and monument conservators. They defined the main goal of the research as determining the mass of the bell using the proposed novel hybrid approach including classical and precise modern geodetic measurements, laser scanning technology and advanced microstructural analyses (also analyses of chemical composition). To achieve the main objective, the following intermediate objectives were identified and implemented during the research:

- (1) Geometry measurements and development of a geometric model of the bell (outer and inner surface) using non-contact surveying inventory methods: the classic geodetic measurement method using a Total Station (TS) and the precise and modern Terrestrial Laser Scanning method.
- (2) Statistical evaluation of measurements to determine the actual deviation of the values measured in relation to the developed model and to evaluate the results. Parametric tests were used to verify the parametric hypotheses: T , T_2 , T_3 and F , assuming the significance level $\alpha=0.05$.
- (3) Analysis of the chemical composition of the historic bell using traditional (optical microscopy) and modern microscopic techniques (scanning electron microscope, glow discharge optical emission spectroscopy) to determine the average density of the bronze.

The rest of the article is organized as follows: in "Results and discussion" we present the research methods, in "Results and discussion" we describe the results of the research and a discussion of the results, and "Conclusion" includes a summary of the research. The course of the research using the hybrid approach to determine the mass of the bell is illustrated in Fig. 1.

Materials and methods

Case study

The bell "Urban" is one of the largest historical bells in Poland (Fig. 2a). It is hung on the church tower in Krosno (Poland) together with two other bells: "Jan" and "Maryan" (Fig. 2b). Its diameter is 1535 mm. The three bells are suspended on a supporting steel structure using

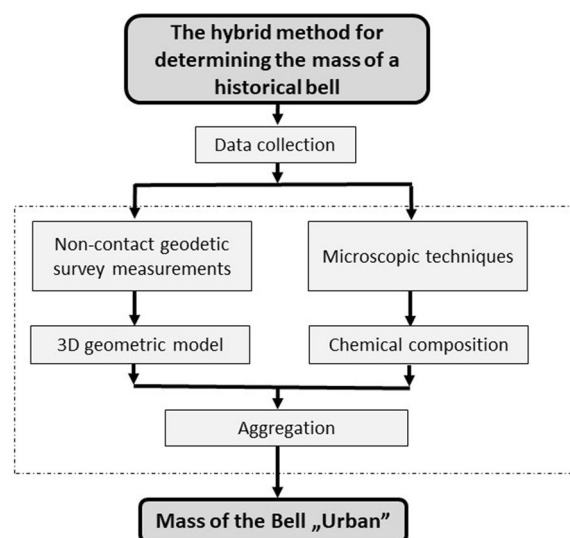


Fig. 1 A flowchart of the research according to the proposed novel hybrid method



Fig. 2 a Bell "Urban", general view. b Bells and their supporting structure in the belfry of the parish church in Krosno, Poland

steel yokes. In theory, based on historical sources [62], the total mass of the bells is estimated at about 4200 kg. Only the bells “Zygmunt” from the Wawel Cathedral in Krakow and “Tuba Dei” from St. Johns’ Cathedral in Toruń are bigger. The bell “Urban” is very rich in architectural detail. The details of the ornaments are delicate but very expressive. On its bell there are two 6 cm high friezes with a motif of lilies, anthems and acanthus leaves. Between them there is an inscription in Latin “SANCTA TRINITAS DEUS MISERERE NOBIS A.D. 1639” (Holy Trinity, God have mercy on us 1639). The lower frieze circling the bell is decorated with campanulas suspended below and closed on the sides with acanthus leaves. There are two plaques on the bell. One with a depiction of the Holy Trinity (dimensions 22×18 cm) is signed with the bell founders’ inscription: “DEI AU XILIO STEPHANUS MEUTEL ET GEORGI OLIVIER ME FECERUNT” (Stefan Meutel and Jerzy Olivier cast me with God’s help). The other plaque shows Robert Wojciech Portius’ mark, containing three stars, a book, a sword, a merchant’s ell (dimensions 16×14 cm) and the abovementioned foundation inscription. Both friezes with ornamental decorations are closed on the bottom with an astragal and on the top with a half cylinder. A unique element is the crown of the bell, which is shaped in the form of six-pointed bows decorated with a motif of lions’ heads [62, 63].

In order to determine the actual forces transferred to the structure during the swinging of the bell “Urban”, it was necessary to calculate its mass. For this purpose, measurements of its volume and chemical composition were carried out using the proposed in the article hybrid method.

Geometric inventory measurements of the bell “Urban”

The TLS method and geodetic tacheometric measurements were used to perform inventory measurements of the outer and inner surface of the bell. A FARO Focus 3D laser scanner was used to perform a 3D scan of the internal and external surface of the bell. This is a phase scanner that can measure up to 1 million points per second (in low resolution mode). The manufacturer of the device does not provide full data on the accuracy of determining the position of a single point in 3D space, only the measurement error for distance, which is ± 2 mm at a range of up to 25 m. A Faro Focus is a relatively small and light device that can be regarded as the basic model for terrestrial 3D laser scanning. The scanning was performed from six scanner stations with a resolution of 6 mm/10 m. Each scanning procedure took approximately 10 min (Fig. 3).

The scans were initially processed with Faro SCENE software. Then, using 6 reference spheres (Fig. 3a), the

point clouds from single scans were combined into a full point cloud reflecting the entire object (Fig. 4).

Tacheometric measurements were performed with a Trimble M3 Total Station in mirrorless distance measurement mode. This total station has an angle accuracy of $\pm 1''$ and a distance accuracy of ± 3 mm.

The outer surface of the bell was measured from 3 positions (two of them are visible in Fig. 3a, b, respectively). The measurement results were transformed to a common coordinate system determined by 5 adjustment points. The adjustment points were marked with targets attached temporarily to the walls of the belfry. The first attempt to measure the inner surface of the bell was unsuccessful. The instrument was not able to measure that surface. A probable cause was the technical limitations of mirrorless measurements, such as the angle of incidence of the beam and the ability of the surface to reflect it [64–66], or too short a distance to the object measured [67]. Another attempt was successful and took place after changing the position of the instrument. The measurement of the internal surface was performed from one stand.

Microstructure and chemical composition analysis using microscopic techniques

The properties of metals and alloys used to make bells, including density, depend on the construction of their internal structure, i.e. macro and microstructural characteristics. For this reason, the purpose of subsequent research was to determine the chemical composition of the alloy and to analyse its microstructure. Unfortunately, microscopy techniques are invasive methods that require cutting out a fragment of the material for testing. The fragment should be much larger than the sample examined under a microscope because the sample has to be cut out in a special device that ensures that the material is cooled to a degree that prevents its structure from changing while it is being cut. Moreover, the key issue is to ensure that samples are representative of the structure, i.e. selected at random. However, in this case, due to the historical construction of the bell, the wear and damage to the clapper, and to minimize interference with the structure, the test samples were obtained only from the damaged clapper. Usually bells are made of bronze, and bell clappers are made of steel. Although the alloys used to make bells must measure up to current standards and obtain characteristics that give them considerable durability, field observations confirm the occurrence in Poland of bells whose bell and heart were made of the same material, which unfortunately characterizes them with poor musical qualities. In the considered case, the damaged clapper was made of bronze in a steel casing. Making such a clapper involved forcing liquid bronze into a hole in the steel casing. Since the clapper was hung

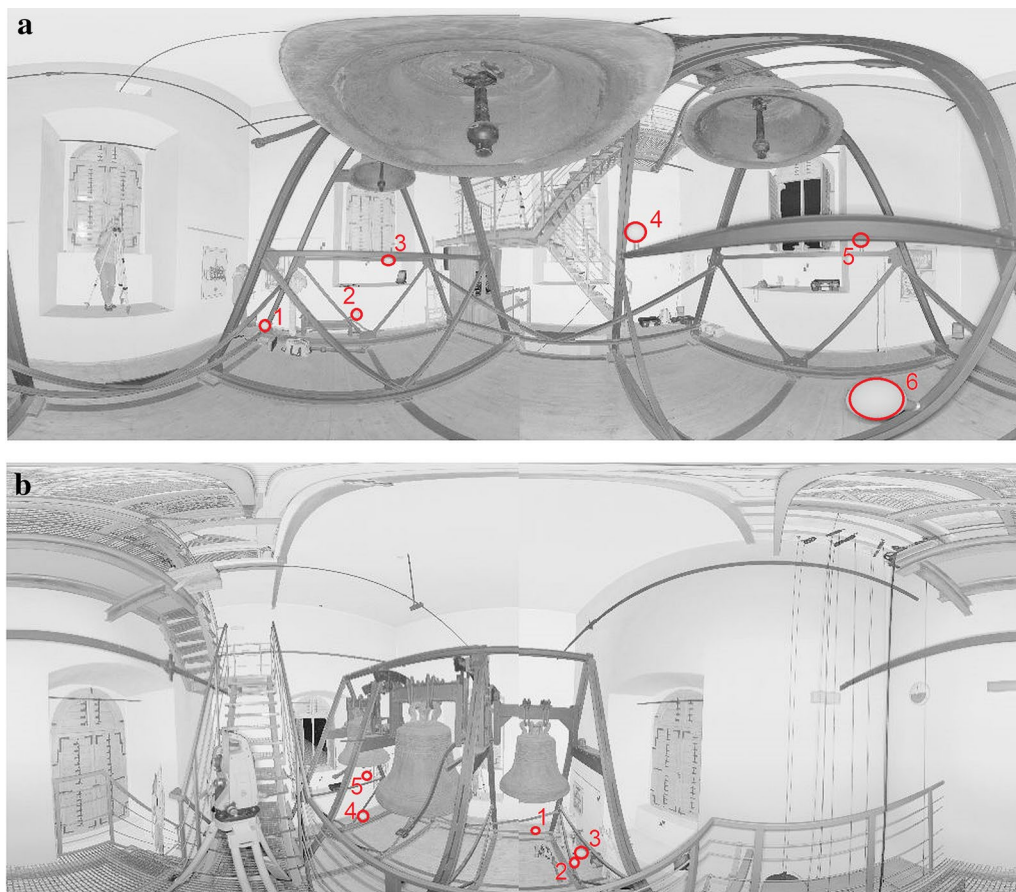


Fig. 3 Examples of scan preview from Faro Focus 3D with visible positions for tacheometric measurements and laser scanner reference spheres marked with red circle: **a** scanning the inner surface of the bell, **b** scanning the outer surface of the bell

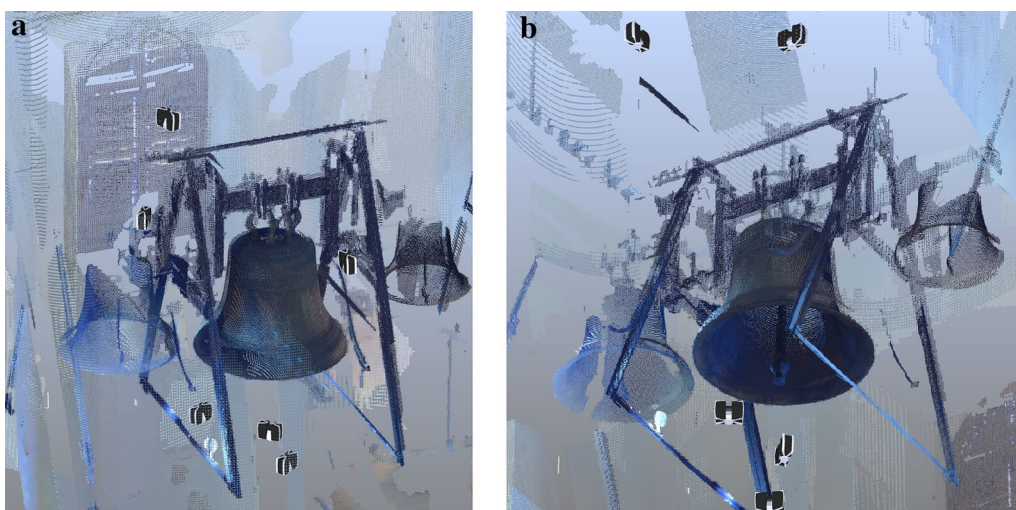


Fig. 4 Point cloud from the combined scans inside the belfry, visible scanner stations marked with the instrument symbol: **a** top view, **b** bottom view

on an Urban bell, the authors assumed in their research that it was part of that bell and made of the same material. Spectral analysis of the chemical composition carried out with a LECO GDS500A optical spectrometer with a glow discharge made it possible to determine the quantitative elemental composition of the alloy. Based on stoichiometric calculations, this test determined the grade of the material in relation to the materials used in the past and the density of the alloy.

Results and discussion

Geodetic measurements of the bell

Due to slight deficiencies in the set of points reflecting the outer surface and insufficient information about the precision of mapping of the bell and its clapper, it was decided to model the data set using manual interpolation of the outer and inner surfaces of the bell. AutoCAD software was used to filter points, separate the object tested and specify both surfaces of the bell separately (Fig. 5).

The shape of the bell was interpolated using circular sections in a horizontal projection. These cross-sections were made on the basis of diameters determined from a vertical projection oriented in six directions (each time

the vertical projection of the point cloud was rotated by 30°). Subsequently, a spatial surface was stretched on the cross-sections (Fig. 6) and the volume of the thus formed solid was determined.

For the point cloud obtained by terrestrial laser scanning, it was possible to create an average of 35 cross-sections, which gave an average density of 3.5 cm at the height of the bell. Due to the smaller set of points obtained from geodetic tachometric measurements, the number of cross-sections for the outer and inner surfaces of the bell in each direction oscillated around 20, i.e. on average one cross-section per every 6 cm at the height of the bell. In this way, 4 solids were created, two limited by the external and two by the internal surfaces of the bell, in both cases, one for each measurement method.

The volume of the bell was determined from the difference between the volume of the solid limited by the surface of the outer and the surface of the inner of the bell. The results are presented in Table 1.

The terrestrial laser scanning method gave the results of the volume of the bell as 0.215 m³, and the geodetic total station measurements as 0.217 m³. It can be noticed that the results of surface interpolation given by the total

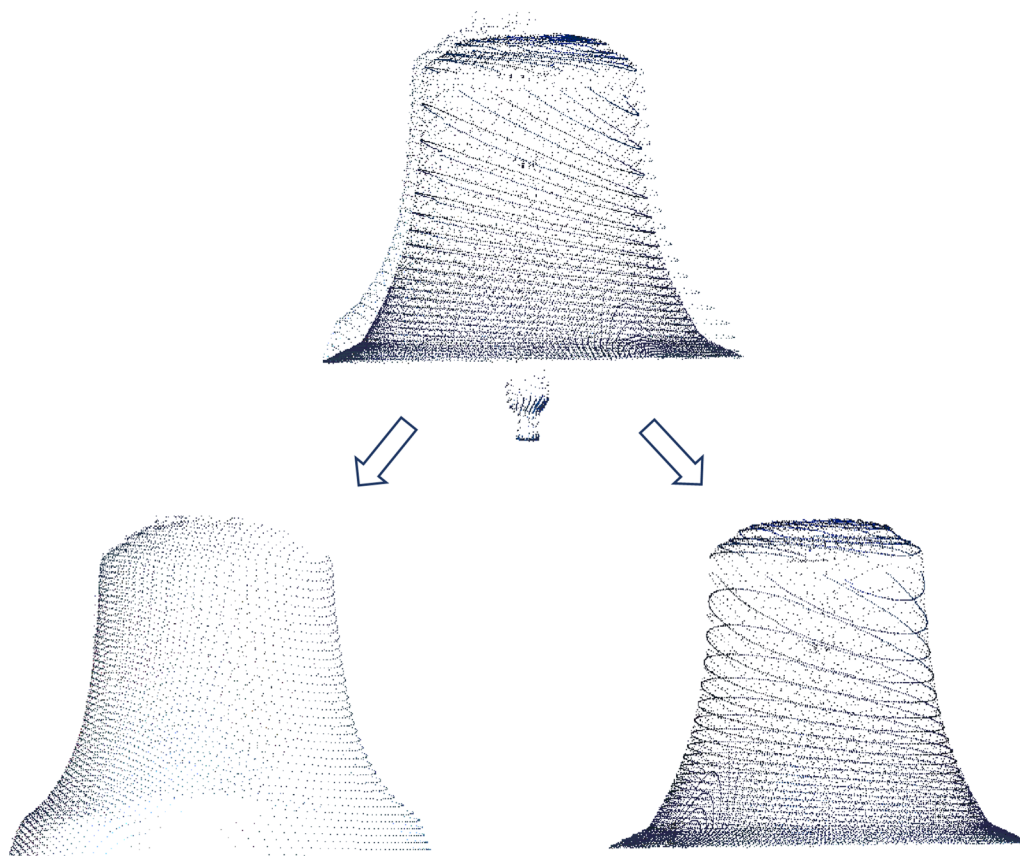


Fig. 5 Point cloud of the whole object and division into the external and internal parts of the point cloud

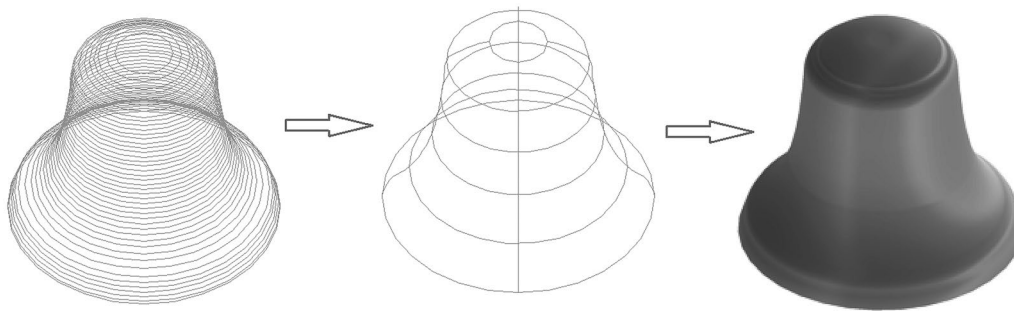


Fig. 6 Example of cross-sections of the bell, the surface stretched on them and the solid

Table 1 Comparison of the results of volume measurements for the outer and inner surface of the bell

No.	Volume measurement – total station		Volume measurement – TLS	
	Outer surface [m ³]	Inner surface [m ³]	Outer surface [m ³]	Inner surface [m ³]
1	1.040	0.839	1.046	0.826
2	1.057	0.831	1.051	0.834
3	1.043	0.833	1.040	0.836
4	1.054	0.826	1.044	0.831
5	1.052	0.824	1.047	0.828
6	1.043	0.835	1.039	0.826
Average value	1.048	0.831	1.045	0.830
Standard deviation	0.007	0.006	0.005	0.005

station measurements are subject to a slightly greater uncertainty (higher standard deviation values Table 1). This was most likely caused not by the accuracy of the measurements, but by the lower density of the measurement points reflecting the surface measured.

The volume values obtained using the total station method and TLS were compared using parametric tests for the average value and variance. In the test *T3* the statistical value was calculated according to the formula:

$$T3 = \frac{\bar{d} \cdot \sqrt{n}}{S_d^*} \quad (1)$$

where: $\bar{d}=0.003 \text{ m}^3$ —average from the differences between the measurements of the respective cross-sections obtained from both measurements, $S_d^*=0.012 \text{ m}^3$ —standard deviation for differences between the TLS and the total station measurements, $n=12$ —number of both samples.

Therefore, at the assumed significance level of $\alpha=0.05$, the volumes determined using both measurement

methods do not differ significantly. To test the hypothesis in relation to volume, the test *T2* was used.

At the assumed significance level of $\alpha=0.05$, the volumes determined using both measurement methods do not differ significantly. Therefore, the target volume of the bell can be determined as the arithmetic mean from both methods, i.e. 0.216 m^3 .

The F test was used for the analysis of variance. At the assumed significance level of $\alpha=0.05$, the values of volume variance calculated using both measurement methods are comparable. Despite the statistically confirmed lack of significant differences in the accuracy of volume determination using both methods, the advantage of the laser scanning method over the classic geodetic measurements is that a much larger data set can be collected in a shorter time. Based on the measurements carried out using the two measurement techniques: TS and TLS, and statistical analyses, the target volume of the bell can be determined as the arithmetic mean from both measurement methods, i.e. 0.216 m^3 .

Material examination using microscopic techniques

The material was examined based on samples taken from the damaged clapper of the bell. A spectral analysis of the chemical composition was performed using a LECO GDS500A optical spectrometer with a glow discharge. Thus, the quantitative elemental composition of the bell alloy was determined. On the basis of the samples, the average percentage chemical composition of the bell alloy was also determined. The measurement results are shown in Fig. 7.

The analysis of chemical composition showed that the content of copper was 78.33% and tin 15.20%. The level of lead in the alloy is relatively high and amounts to 2.84%. The other elements are impurities and their content is respectively: 0.41%—Ni; 0.15%—Ag; 2.69%—Sb (Fig. 7). Since it was not possible to conduct invasive tests (the structure is listed), the other properties of the tin bronze were determined using information from available

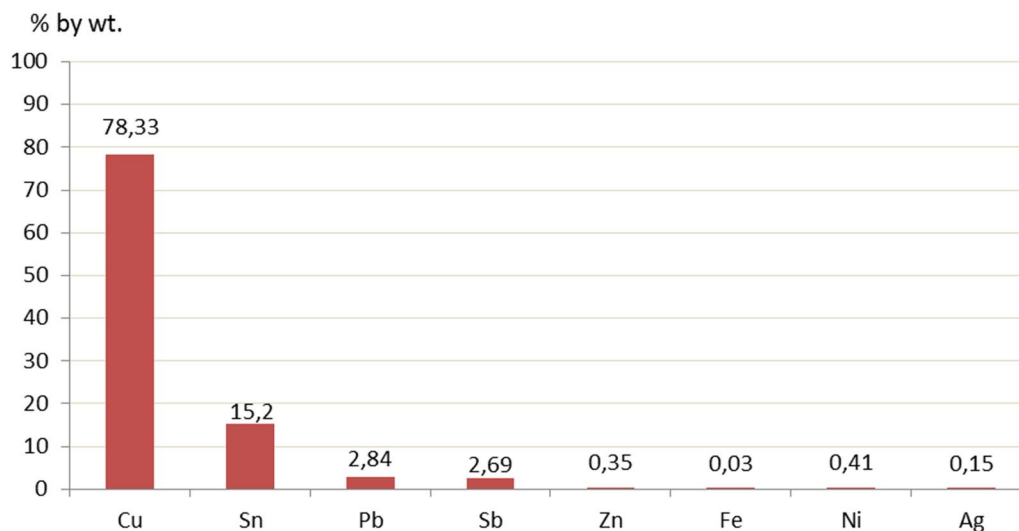


Fig. 7 Average chemical composition of the bronze used for the bell "Urban" [%]

literature [68]. Based on comparison with the data provided in [69], the hardness of the tin bronze can be estimated at approximately 180 in the Brinell scale (HB), the tensile strength value is 330 MPa, and the yield point is 280 MPa.

In study, the structure of the alloy was analysed using an optical microscope (Fig. 8) and a scanning electron microscope (Tables 2, 3) to determine the size and distribution of solid and gaseous inclusions. Microscopic observations showed the presence of inclusions in the alloy (Fig. 8). The inclusions were distributed in the structure unevenly and formed clusters (Fig. 8), some of them were heterogeneous (Tables 2, 3).

Scanning electron microscopy (SEM) combined with the EDS technique made it possible to microanalyse the elemental composition of the surface of the samples (Tables 2, 3). The location of the measurement points together with the visible impurities and inclusions on the sample taken for testing are shown in Tables 2 and 3. The tests were performed at two magnifications: $\times 530$ and $\times 800$. For $\times 530$ magnification, 6 measurement points were selected on the test sample. For measurement point 6, the tests were also carried out at $\times 800$ magnification, and another 3 measurement subpoints were selected for testing. Table 2 shows the chemical composition in individual places with visible solid and gaseous inclusions at $\times 530$ magnification, and Table 3 at $\times 800$ magnification.

The analyses indicated many gaseous inclusions: oxygen (Tables 2, 3) and non-metallic inclusions: carbon and sulphur (Table 2). The high level of carbon may indicate the original method of smelting the alloy. This is most likely a remnant of the charcoal used as fuel

during the smelting process. Inclusions of zinc, antimony (stibium) (Table 2) and lead (Table 3) were also detected. It is assumed that "resonant" bronze for bells is most often a two-component alloy of copper and tin with a tin content of 18–22%. Observations of the microstructure indicate the old bronze recipe, in which the ratio of copper to tin is 5:1 [69]. Figure 9 shows the position of the chemical composition of the material used for the bell "Urban" on a copper-tin equilibrium diagram [69–71].

Based on Fig. 9, it is possible to analyse the phase transformations of the alloy and to understand the process of its solidification. Solidification begins at the temperature defined by point *A* and ends at the temperature defined by point *B*. After solidification, the alloy has a structure consisting of phase α (a solid solution of tin in copper containing up to 15.2% Sn) and phase β (an intermediate electronic phase containing 22.0–26.0% Sn). The analyses of the chemical composition made it possible to determine the share of individual elements and, above all, to calculate the average density of the bronze. The density of the bronze was determined assuming additivity, i.e. the density of bronze is equal to the sum of the product of the share of individual elements (according to Fig. 7) and their density in the alloy (Table 4). In this case, the average density of the bronze is $8.677 \text{ g}\cdot\text{cm}^{-3}$.

The density value obtained was compared with the density value found in literature [72], which said that the density of metal classified as bronze could be assumed as $8.800 \text{ g}\cdot\text{cm}^{-3}$. To verify if the average density obtained from the tests was in compliance with the value found in literature, a parametric test for the average value was used—the test *T*.

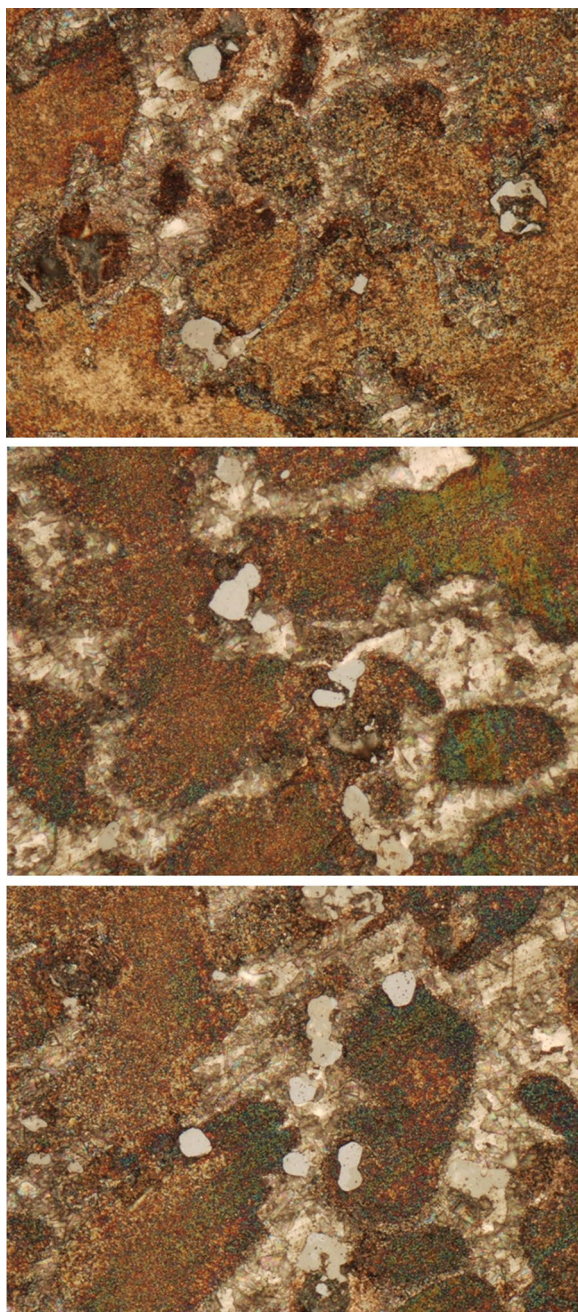


Fig. 8 Image of the samples obtained using an optical microscope at $\times 500$ magnification

Based on the test of the hypothesis at the assumed significance level of $\alpha = 0.05$, and the density of the bronze determined during the research, it can be concluded that this density value is significantly different from the value of $8.800 \text{ g}\cdot\text{cm}^{-3}$ found in literature. The tests conducted on the hypothesis for the average density confirm that tin bronze in terms of its physical characteristics, in this case density, is different in each historical bell, and

information about this material found in literature may not always be reliable. They also confirm that although the use of the additive method for density calculations is an approximate approach, it is sufficient for structural and construction analyses.

Determination of the mass of the bell and discussion of the results

Based on the geodetic measurements and chemical tests, the volume and density of the bell were determined, which made it possible to determine its mass: $m = 0.216 \text{ m}^3 \cdot 10^6 \text{ cm}^3 \cdot 8.677 \text{ g}\cdot\text{cm}^{-3} = 1872.07 \text{ kg}$. The weight of the damaged clapper of the bell is 65.52 kg. The total weight of the bell, including the clapper, is 1937.59 kg. The authors also attempted to determine the mass of the bell on the basis of dynamic tests, for which a portable Scadas Mobile analyzer and one acceleration sensor were used. The results were similar, however, due to the clapper damage, it was decided that it would be more advantageous to use the proposed hybrid method.

To this day, tin is used for making bronze and constitutes 15–20% of its weight. The share of harder, high-tin phases in the structure of the alloy affects the tone and sound of a bell. For this reason, the materials used in the past to cast bells were characterized by individual properties that guaranteed their characteristic and unique sound. Despite attempts to replace rare and expensive tin with other elements, it has not been possible to obtain an alloy with similar sound properties. At this point, it is worth emphasizing that bronzes containing less tin have lower hardness and greater plasticity, and for this reason, they are resistant to all kinds of impacts. Bronzes containing a higher admixture of tin are harder and more brittle.

In the samples obtained from the bell, apart from the content of copper (78.33%), tin (15.20%) and lead (2.84%), there are also contents of other elements that are impurities. For example, there is a relatively high content of antimony (2.69%). At present, antimony is considered to be a harmful impurity that makes alloys brittle. Lead (2.89% in the tested material) is also considered an undesirable admixture because it does not dissolve in bronze and forms separate inclusions that increase the ability of the material to damp vibrations. However, using the bell casting technique of the time (seventeenth century), it is not possible to avoid such defects. The metallurgical research conducted in this case indicates that the bell "Urban" represents a high level of 17th-century bell founding technology. At this point, it is worth quoting the results of analyses of the chemical composition of materials from other bells located in various parts of the world available in literature and comparing them with the results obtained in

Table 2 SEM EDS image of the sample at ×530 magnification with marked measurement points and the chemical composition of the samples at individual measurement points

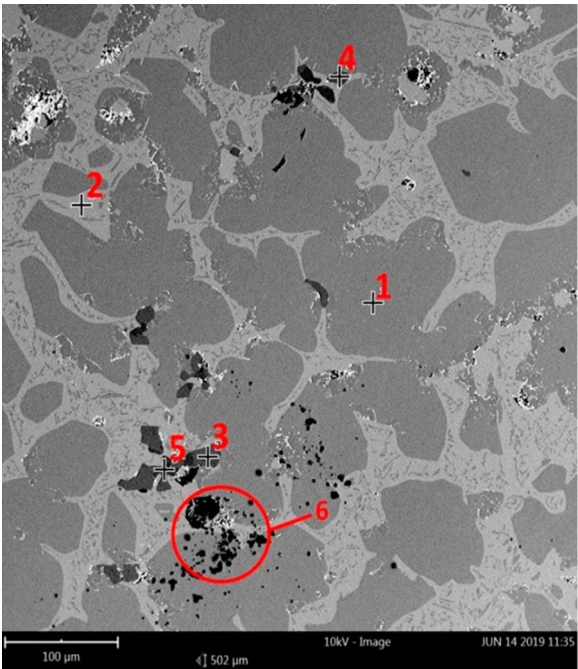
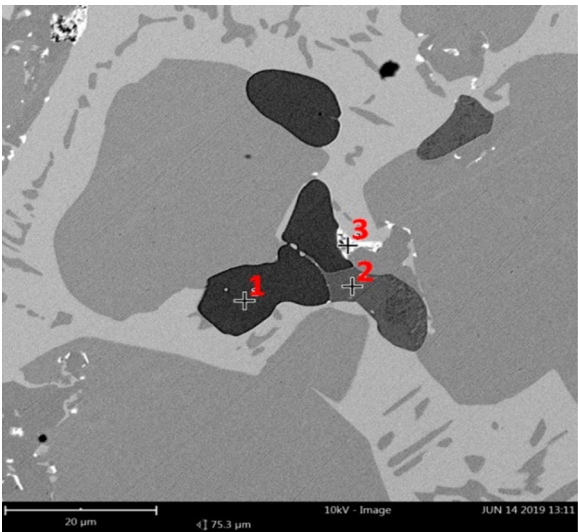
	Measurement point number	Element	% of atomic mass
	1	Cu	21.43
		C	70.36
		Sn	1.77
		O	6.44
	2	Cu	28.54
		C	6.34
		Sn	57.87
		O	7.25
	3	Cu	24.76
		C	64.84
		Sn	6.37
		O	3.84
		Sb	0.19
	4	Cu	28.88
		C	63.68
		S	7.44
	5	Zn	24.46
		C	57.29
	S	13.12	
	Cu	2.88	
	O	2.25	

Table 3 SEM EDS image of measurement point No. 6 with marked measurement subpoints at ×800 magnification and the chemical composition of the samples at individual measurement subpoints of measurement point No. 6

	Measurement point number	Element	% of atomic mass
	1	C	75.57
		Zn	12.53
		Cu	3.56
		S	5.12
		O	3.22
	2	Cu	17.75
		C	75.99
		S	3.79
		O	2.47
	3	Pb	9.94
		C	64.53
		Cu	7.85
		O	17.00
		Sn	0.68

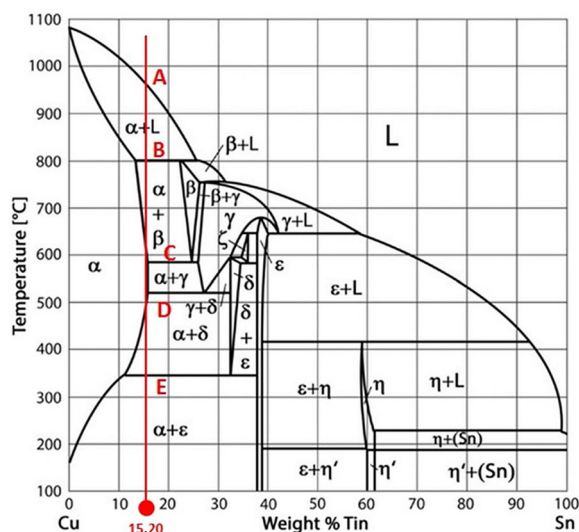


Fig. 9 Copper-tin equilibrium diagram of the material used for the bell "Urban"

this case [72–74]. The comparison is shown in Table 5. A similar content of tin as in the bell "Urban" was found in the material of the bell from Japan dating back to the eighth century. The other bells listed in Table 5 were made of materials containing different contents of tin.

Conclusions

During the conservation of historic buildings, it is advisable to measure the physical and chemical properties of their elements using methods that are as little invasive to their structure as possible. For this reason, the authors of the research proposed an interdisciplinary hybrid approach to determine the mass of the historic bell "Urban", combining non-contact measurements of the geometry of the object with geodetic methods and chemical material tests.

The use of tacheometry and terrestrial laser scanning (TLS) enabled non-contact measurements of the geometry of the outer and inner of the bell, construction of its 3D model and eventually calculation of the volume of the bell. It should be emphasized that the results of the interpolation of the surface of the bell from tacheometric measurements are subject to a slightly greater uncertainty, which probably results from the lower density of measurement points. The values of the volume of the bell obtained with both methods were compared using statistical parametric tests for the mean value and variance. It was shown that at the assumed significance level of $\alpha=0.05$, the volumes determined using both measurement methods did not differ significantly. Finally, the volume of the bell was determined as the arithmetic mean of both measurement methods, which was 0.216 m^3 .

Table 4 Results for the density of the bronze

	Element/Calculation value	Cu	Sn	Pb	Sb	Zn	Fe	Ni	Ag
(1)	Average Content of elements in the bronze for 6 determinations [-]	0.7833	0.152	0.0284	0.0269	0.0035	0.0003	0.0041	0.0015
(2)	Element density [$\text{g}\cdot\text{cm}^{-3}$]	8.92	7.29	11.34	6.69	7.14	7.87	8.91	10.49
(3)	Product: (1) \times (2)	6.9870	1.1081	0.3221	0.1800	0.0250	0.0024	0.0365	0.0157
Bronze density [$\text{g}\cdot\text{cm}^{-3}$]: sum of the values from line (3)		8.677							

Table 5 Chemical composition of the tested material compared with other cases. Prepared by the authors, based on [74]

Country/time of manufacture	Content of elements [%]							
	Cu	Sn	Zn	Sb	Pb	Ni	Fe	Other
Poland, bell Urban, 17th c	78.33	15.20	0.35	2.69	2.84	0.41	0.03	0.15 Ag
China, 1110-221 BC		17.45	0.08		8.46	0.03		
Japan, 8th c		15.45		8.32	5.63	1.35		
England, 10th c.		18.75			4.35	1.00		
Russia, Tsar-kolokol bell, 18th c	84.51	13.91						1.25 S
Korean Sangwonsa bell 8th c	83.87	13.26	0.32		2.12			
Japan, Japanese bell, 20th c	82.10	9.00–13.00	1.00–1.70					
USA, Los Angeles, 20th c	86.07	13.3	0.14	0.01	0.08		0.07	

Extensive chemical research, in this case in the field of metallurgy, carried out using modern microscopic techniques, made it possible to determine the essential characteristics of the material used to cast the bell and to formulate conclusions about the conditions in which it had been cast. It was found that apart from the content of copper (78.33%), tin (15.20%) and lead (2.84%) the material of the bell contained other impurities, e.g. antimony and lead. Scanning electron microscopy combined with the EDS technique enabled microanalysis of the elemental composition of the surface of the samples and showed many gaseous and non-metallic inclusions. The determination of the chemical composition and the share of individual elements made it possible to calculate the average density of the bronze. The density of the bronze was determined assuming additivity (the density of bronze is equal to the sum of the product of the share of individual elements and their density in the alloy). In this case, the average density of the bronze is $8.677 \text{ g}\cdot\text{cm}^{-3}$. The proposed hybrid method, made it possible to determine the volume of the bell and the density of the material without the need to dismantle the bell. Thus, the mass of the bell was determined, which was the goal of the research. The mass of the bell is 1872.07 kg, and including the damaged clapper it is 1937.59 kg. It should be emphasized that microscopic examinations were performed on samples from the damaged clapper. The results of the detailed examination of the chemical composition of the samples are very important, also in terms of repair work since they can contribute significantly to the reconstruction of the clapper and also enable other repairs or conservation work in a way that is safe for the research object. Moreover, the use of laser scanning enabled the construction of a spatial model that can complete the conservation documentation of the bell and facilitate possible conservation work in the future.

Based on the conducted research, we propose a novel hybrid method as a tool to be used by practitioners. Both the proposed method and the review of the state of the art can then be used to determine the mass of bells (also during conservation work assessing the degree of wear of materials), with accuracy that meets the requirements of the work, as evidenced by an example of the analysis.

Abbreviations

BIM	Building information modelling
EDS	Energy dispersive X-ray spectroscopy
GIS	Geographic information system
GNSS	Global Navigation Satellite Systems
GDOES	Glow discharge optical emission spectroscopy
HBIM	Historical building information modelling
LiDAR	Light detection and ranging
OM	Optical microscopy

TLS	Terrestrial laser scanning
TS	Total station
SEM	Scanning electron microscope

Acknowledgements

The authors gladly acknowledge the director and employees of the Museum of Crafts in Krosno for providing the bell for research.

Author contributions

IS, AL and MM Conceptualization, Methodology, Formal analysis, Writing—original draft. GO, MR and MO: Methodology, Data curation, Formal analysis, Writing—original draft, Visualization. All authors read and approved the final manuscript.

Funding

This work stems from the research supported by the subsidies for maintenance and development of research potential awarded by the Ministry of Education and Science in Poland for the Rzeszów University of Technology, the Cracow University of Technology and the University of Zielona Góra.

Availability of data and materials

The datasets used and/or analyzed during the current study are available from the corresponding author on reasonable request.

Declarations

Ethics approval and consent to participate

Not applicable.

Consent for publication

Not applicable.

Competing interests

The authors declare that they have no competing interests.

Received: 4 May 2023 Accepted: 22 July 2023

Published online: 26 July 2023

References

- Croce P. Nonlinear dynamics of swinging clapper bells under arbitrary or resonant forcing functions. *Appl Sci.* 2020;10:5528. <https://doi.org/10.3390/app10165528>.
- Woodhouse J, Rene JC, Hall CS, Smith LTW, King FH, McClenahan JW. The dynamics of a ringing church bell. *Adv Acoust Vib.* 2012;2012:1–19. <https://doi.org/10.1155/2012/681787>.
- Vincenzi L, Bassoli E, Ponsi F, Castagnetti C, Mancini F. Dynamic monitoring and evaluation of bell ringing effects for the structural assessment of a masonry bell tower. *J Civ Struct Heal Monit.* 2019;9:439–58. <https://doi.org/10.1007/s13349-019-00344-9>.
- Ivorra S, Palomo M, Verdú G, Zasso A. Dynamic forces produced by swinging bells. *Meccanica.* 2006;41:47–62. <https://doi.org/10.1007/s11012-005-7973-y>.
- Bachmann H, et al. Vibration problems in structures. In: Practical guidelines. Birkhauser Verlag; 1995.
- Rapp P. Historical bells – mechanics and drive problems. *Journal of Heritage Conservation.* 2014;40:41–57.
- Nowogońska B. Consequences of improper renovation decisions in a 17th century half-timbered building. *Sci Rev Eng Environ Sci.* 2021;29(4):557–66. <https://doi.org/10.22630/PNIKS.2020.29.4.48>.
- Burzyński T, Perlikowski P, Balcerzak M, Brzeski P. Dynamics loading by swinging bells—Experimental and numerical investigation of the novel yoke–bell–clapper system with variable geometry. *Mech Syst Signal Process.* 2022;180:109429. <https://doi.org/10.1016/j.ymssp.2022.109429>.

9. Ivorra S, Pallarés FJ, Adam JM. Masonry bell towers: dynamic considerations. *Proc Inst Civil Eng Struct Build*. 2011;164(1):3–12. <https://doi.org/10.1680/stbu.9.00030>.
10. Bru D, Ivorra S, Betti M, Adam JM, Bartoli G. Parametric dynamic interaction assessment between bells and supporting slender masonry tower. *Mech Syst Signal Process*. 2019;129:235–49. <https://doi.org/10.1016/j.ymssp.2019.04.038>.
11. Foti D, Ivorra S, Diaferio M, Bru D, Vacca V. Resonances detected on a historical tower under bells' forced vibrations. *Frattura ed Integrità Strutturale*. 2018;12(46):203–15. <https://doi.org/10.3221/GF-ESIS.46.19>.
12. Kadaj R. Models, methods and computational algorithms of kinematic networks in geodetic measurements of displacements and deformations of objects (in Polish). Poland, Kraków: Publishing House of the Agricultural University; 1998.
13. Nikulishyn V, Savchyn I, Lompas O, Lozynskiy V. Applying of geodetic methods for monitoring the effects of waste-slide at Lviv municipal solid waste landfill. *Environ Nanotechnol Monit Manage*. 2020;13:100291. <https://doi.org/10.1016/j.enmm.2020.100291>.
14. Gołuch P, Kuchmister J, Ćmielewski K, Bryś H. Multi-sensors measuring system for geodetic monitoring of elevator guide rails. *Measurement*. 2018;130:18–31. <https://doi.org/10.1016/j.measurement.2018.07.077>.
15. Donggun K, Younghak K, Hoon S. Accelerated cable-stayed bridge construction using terrestrial laser scanning. *Autom Constr*. 2020;117:10326. <https://doi.org/10.1016/j.autcon.2020.103269>.
16. Sztubecki J, Topoliński S, Mrówczyńska M, Bağrıçık B, Beycioğlu A. Experimental research of the structure condition using geodetic methods and crackmeter. *Appl Sci*. 2022;12(13):6754. <https://doi.org/10.3390/app12136754>.
17. Marsella M, Nardinocchi C, Paoli A, Tini MA, Vittuari L, Zanutta A. Geodetic measurements to control a large research infrastructure: the Virgo detector at the European Gravitational Observatory. *Measurement*. 2020;151:107154. <https://doi.org/10.1016/j.measurement.2019.107154>.
18. Bryn MJ, Afonin DA, Bogomolova NN. Geodetic monitoring of deformation of building surrounding an underground construction. *Proc Eng*. 2017;189:386–92. <https://doi.org/10.1016/j.proeng.2017.05.061>.
19. Hohensinn R, Häberling S, Geiger A. Dynamic displacements from high-rate GNSS: Error modeling and vibration detection. *Measurement*. 2020;157:107655. <https://doi.org/10.1016/j.measurement.2020.107655>.
20. Wójcik A, Kłapa P, Mitka B, Piech I. The use of TLS and UAV methods for measurement of the repose angle of granular materials in terrain conditions. *Measurement*. 2019;146:780–91. <https://doi.org/10.1016/j.measurement.2019.07.015>.
21. Shevchuk V, Burshtynska K, Korolik I, Halochkin M. Monitoring of horizontal displacements and changes of the riverine area of the Dniester River. *J Water Land Dev*. 2021;49(IV–VI):1–15. <https://doi.org/10.24425/jwld.2021.137091>.
22. Li M, Li M, Rem Q, Li H, Song L. DRLSTM: a dual-stage deep learning approach driven by raw monitoring data for dam displacement prediction. *Adv Eng Informat*. 2022;51:101510. <https://doi.org/10.1016/j.aei.2021.101510>.
23. Golparvar-Fard M, Bohn J, Teizer J, Savarese S, Peña-Mora F. Evaluation of image-based modeling and laser scanning accuracy for emerging automated performance monitoring techniques. *Autom Constr*. 2011;20:1143–55. <https://doi.org/10.1016/j.autcon.2011.04.016>.
24. Suchocki C, Katzer J. Terrestrial laser scanning harnessed for moisture detection in building materials—problems and limitations. *Autom Constr*. 2018;94:127–34. <https://doi.org/10.1016/j.autcon.2018.06.010>.
25. Bieda A, Bydłoz J, Warchoła A, Balawejder M. Historical underground structures as 3D cadastral objects. *Remote Sensing*. 2020;12(10):1547. <https://doi.org/10.3390/rs12101547>.
26. Vlaeyen M, Haitjema H, Dewulf W. Virtual task-specific measurement uncertainty determination for laser scanning. *Precis Eng*. 2023;80:208–28. <https://doi.org/10.1016/j.precisioneng.2022.12.008>.
27. Wang J, Qin Q, Bai Z. Characterising the effects of opencast coal-mining and land reclamation on soil macropore distribution characteristics using 3D CT scanning. *CATENA*. 2018;171:212–21. <https://doi.org/10.1016/j.catena.2018.07.022>.
28. Török A, Bögöly G, Somogyi A, Lovas T. Application of UAV in topographic modelling and structural geological mapping of quarries and their surroundings—delineation of fault-bordered raw material reserves. *Sensors*. 2020;20:489. <https://doi.org/10.3390/s20020489>.
29. Li J, Yang B, Cong Y, Cao L, Fu X, Dong Z. 3D forest mapping using a low-cost UAV laser scanning system: investigation and comparison. *Remote Sens*. 2019;11(6):717. <https://doi.org/10.3390/rs11060717>.
30. Bochenska A, Markiewicz J, Łapiński S. The combination of the image and range-based 3d acquisition in archaeological and architectural research in the royal castle in Warsaw, International Archives of the Photogrammetry. *Remote Sens Spatial Inform Sci*. 2019;XLII-2/W15:177–84. <https://doi.org/10.5194/isprs-archives-XLII-2-W15-177-2019>.
31. Skrzypczak I, Oleniacz G, Leśniak A, Zima K, Mrówczyńska M, Kazak JK. Scan-to-BIM method in construction: assessment of the 3D buildings model accuracy in terms inventory measurements. *Build Res Informat*. 2022;50(8):859–80. <https://doi.org/10.1080/09613218.2021.2011703>.
32. Wang Q, Tan Y, Mei Z. Computational methods of acquisition and processing of 3D point cloud data for construction applications. *Arch Comput Methods Eng*. 2020;27:479–99. <https://doi.org/10.1007/s11831-019-09320-4>.
33. Błaszczak-Bąk W, Suchocki C, Mrówczyńska M. Optimization of point clouds for 3D bas-relief modeling. *Automat Constr*. 2022;140:104352. <https://doi.org/10.1016/j.autcon.2022.104352>.
34. Wałach D, Kaczmarczyk GP. Application of TLS remote sensing data in the analysis of the load-carrying capacity of structural steel elements. *Remote Sens*. 2021;13(14):2759. <https://doi.org/10.3390/rs13142759>.
35. Achakir F, Fkihi SE, Mouaddib EM. Non-Model-Based approach for complete digitization by TLS or mobile scanner. *ISPRS J Photogramm Remote Sens*. 2021;178:314–27. <https://doi.org/10.1016/j.isprsjprs.2021.06.014>.
36. Korumaz M, Betti M, Conti A, Tucci G, Bartoli G, Bonora V, Korumaz AG, Fiorini L. An integrated terrestrial laser scanner (TLS), deviation analysis (DA) and finite element (FE) approach for health assessment of historical structures. A minaret case study. *Eng Struct*. 2017;153:224–38. <https://doi.org/10.1016/j.engstruct.2017.10.026>.
37. Kampczyk A, Dybel K. Integrating surveying railway special grid pins with terrestrial laser scanning targets for monitoring rail transport infrastructure. *Measurement*. 2021;170:108729. <https://doi.org/10.1016/j.measurement.2020.108729>.
38. Yuan L, Guo J, Wang Q. Automatic classification of common building materials from 3D terrestrial laser scan data. *Automat Constr*. 2020;110:103017. <https://doi.org/10.1016/j.autcon.2019.103017>.
39. Barazzetti L, Banfi F, Brumana R, Gusmeroli G, Oreni D, Previtali M, Roncoroni F, Schiantarelli G. BIM from laser clouds and finite element analysis: combining structural analysis and geometric complexity. *Int Arch Photogramm Remote Sens Spatial Inf Sci*. 2015;XL-5/W4:345–50.
40. Quattrini R, Malinverni ES, Clini P, Nespeca R, Orlietti E. From TLS to HBIM. High quality semantically-aware 3D modelling of complex architecture. *Int Arch Photogramm Remote Sens Spatial Inf Sci*. 2015;XL-5/W4:367–74.
41. Siebke I, Campana L, Ramstein M, Furtwängler A, Hafner A, Löscher S. The application of different 3D-scan-systems and photogrammetry at an excavation—a Neolithic dolmen from Switzerland. *Dig Appl Archaeol Cult Herit*. 2018;10:e00078. <https://doi.org/10.1016/j.daach.2018.e00078>.
42. Vorobyev A, Garnier F, van Dijk NP, Hagman O, Gamstedt EK. Evaluation of displacements by means of 3D laser scanning in a mechanically loaded replica of a hull section of the Vasa ship. *Dig Appl Archaeol Cult Herit*. 2018;11:e00085. <https://doi.org/10.1016/j.daach.2018.e00085>.
43. Carvalho M, Debut V, Antunes J. Physical modelling techniques for the dynamical characterization and sound synthesis of historical bells. *Herit Sci*. 2021;9(157). <https://doi.org/10.1186/s40494-021-00620-2>.
44. Gardzińska A. Application of terrestrial laser scanning for the inventory of historical buildings on the example of measuring the elevations of the buildings in the old market square in Jarosław. *Civil Environ Eng Rep*. 2021;2(31):293–300. <https://doi.org/10.2478/ceer-2021-0030>.
45. Kłapa P, Mitka B, Zygmunt M. Integration of TLS and UAV data for the generation of a three-dimensional basemap. *Adv Geodesy Geoinf*. 2022;71(4). <https://doi.org/10.24425/agg.2022.141301>.
46. Yu Z, Zhang L. Design of low wear artificial hip joint considering 3D physiological loading and motion. *Wear*. 2023;523:204744. <https://doi.org/10.1016/j.wear.2023.204744>.
47. Gelderblom HR, Hazelton PR. Specimen collection for electron microscopy. *Emerg Infect Dis*. 2000;6(4):433–4. <https://doi.org/10.3201/eid0604.000427>.
48. Goldstein JI, et al. Scanning electron microscopy and x-ray microanalysis. New York: Springer; 2003.

49. Moropoulou A, Zendri E, Ortiz P, Delegou ET, Ntoutsis I, Balliana E, Becerra J, Ortiz R. Scanning microscopy techniques as an assessment tool of materials and interventions for the protection of built cultural heritage. *Hindawi Scann.* 2018;2019:376214. <https://doi.org/10.1155/2019/5376214>.
50. Ruffolo SA, Comite V, La Russa MF. An analysis of the black crusts from the Seville Cathedral: a challenge to deepen the understanding of the relationships among microstructure, microchemical features and pollution sources. *Sci Total Environ.* 2015;502:157–66. <https://doi.org/10.1016/j.scitotenv.2014.09.023>.
51. Ortiz R, Ortiz P, Vázquez M, Martín JM. Integration of georeferenced informed system and digital image analysis to assess the effect of cars pollution on historical buildings. *Constr Build Mater.* 2017;139:320–33. <https://doi.org/10.1016/j.conbuildmat.2017.02.030.49>.
52. Kurzawska A, Sobkowiak-Tabaka I. *Micropast. Specialist research in archaeology* (in Polish), Adam Mickiewicz University Press, Poznań; 2021. <https://doi.org/10.14746/WA.2021.1.978-83-946591-8-9>.
53. Delaney JK, Zeibel JG, Thoury M. Visible and infrared imaging spectroscopy of Picasso's harlequin mosaic: mapping and identification of artist materials in situ. *Appl Spectrosc.* 2010;64(6):584–94. <https://doi.org/10.1366/000370210791414443>.
54. Daniele V, Taglieri G, Quaresima R. The nanolimes in cultural heritage conservation: characterisation and analysis of the carbonation process. *J Cult Herit.* 2008;9(3):294–301. <https://doi.org/10.1016/j.culher.2007.10.007>.
55. Rodrigues JD, Grossi A. Indicators and ratings for the compatibility assessment of conservation actions. *J Cult Herit.* 2007;8(1):32–43. <https://doi.org/10.1016/j.culher.2006.04.007>.
56. Anselmetti FS, Luthi S, Eberli GP. Quantitative characterization of carbonate pore systems by digital image analysis. *AAPG Bull.* 1998;82(10):1815–36.
57. Cardell C, Yebra A, van Grieken RE. Applying digital image processing to SEM-EDX and BSE images to determine and quantify porosity and salts with depth in porous media. *Microchim Acta.* 2002;140:9–14.
58. Skoulikidis T, Papakonstantinou-Ziotis P. Mechanism of sulphation by atmospheric SO₂ of the limestones and marbles of the ancient monuments and statues: I. observations in situ (Acropolis) and laboratory measurements. *Br Corros J.* 2013;16(2):63–9. <https://doi.org/10.1179/000705981798274986>.
59. Theoulakis P, Moropoulou A. Salt crystal growth as weathering mechanism of porous stone on historic masonry. *J Porous Mater.* 1998;6(4):345–58.
60. Silva AS, Cruz T, Paiva MJ. Mineralogical and chemical characterization of historical mortars from military fortifications in Lisbon harbour (Portugal). *Environ Earth Sci.* 2011;63(7–8):1641–50. <https://doi.org/10.1007/s12665-011-0985-0>.
61. Tenconi M, Karatasios I, Bala'awi F, Kilikoglou V. Technological and microstructural characterization of mortars and plasters from the Roman site of Qasr Azraq, in Jordan. *J Cult Herit.* 2018;33:100–16. <https://doi.org/10.1016/j.culher.2018.03.005>.
62. Rymar M, Ślęczka L. Resistance and durability analysis of steel supporting structure on the bell tower of St Trinity church in Krosno. *J Civil Eng Environ Architect.* 2015;11(62):405–15. <https://doi.org/10.7862/rb.2015.205>.
63. Khalil R. Accuracy evaluation of long-range reflectorless distance measurement3. *Positioning.* 2015;6:61–70. <https://doi.org/10.4236/pos.2015.63007>.
64. Lambrou E, Pantazis G. Evaluation of the credibility of reflectorless distance measurement. *J of Survey Eng.* 2010;136(4):165. [https://doi.org/10.1061/\(ASCE\)SU.1943-5428.0000029](https://doi.org/10.1061/(ASCE)SU.1943-5428.0000029).
65. Świętoń T, Oleniacz G. Accuracy of steel flange measurements in renovation and construction work for offshore industry. *J Survey Eng.* 2020;146(2). [https://doi.org/10.1061/\(ASCE\)SU.1943-5428.0000310](https://doi.org/10.1061/(ASCE)SU.1943-5428.0000310).
66. Trimble M3 DR Series Total Station user Guide; Trimble; 2010.
67. Brunarski L. Conformity criteria for the characteristic strength of building materials in standards PN-EN-ISO (in Polish). *Build Res Inst Quart.* 2002;4(124):15.
68. Lisovskii VA, Lisovskaya OB, Kochetkova LP, Favstov YK. Sparingly alloyed bell bronzes with elevated parameters of mechanical properties. *Met Sci Heat Treat.* 2007;49(5–6):232–5. <https://doi.org/10.1007/s11041-007-0041-6>.
69. Vináš J, Vrabel M, Greš M, Brezina J, Sabadka D, Fedorko G, Molnár V. Restoration of worn movable bridge props with use of bronze claddings. *Materials.* 2018;11:459. <https://doi.org/10.3390/ma11040459>.
70. Shim JH, Oh CS, Lee BJ, Lee DN. Thermodynamic assessment of the Cu-Sn system. *Int J Mater Res.* 1996;87(3):205–12. <https://doi.org/10.1515/ijmr-1996-870310>.
71. Lide DR. *CRC handbook of chemistry and physics.* 85th ed. USA: CRC Press; 2004.
72. Won CS, Jung JP, Won KS, Sharma A. Technological insights into the evolution of bronze bell metal casting on the Korean Peninsula. *Metals.* 2022;12(11):1776. <https://doi.org/10.3390/met12111776>.
73. Yum YH. Bell of Friendship, Bulletin Ministry of Culture and Information Republic of Korea. Department of Design and Production Engineering College of Engineering. Seoul National University, Korea; 1980.
74. Krokosz J, Sękowski K. Metallurgical research of the material of the "Urban" bell from Biecz (in Polish). *Quart J Hist Sci Technol.* 1981;26(2):363–78.

Publisher's Note

Springer Nature remains neutral with regard to jurisdictional claims in published maps and institutional affiliations.

Submit your manuscript to a SpringerOpen® journal and benefit from:

- Convenient online submission
- Rigorous peer review
- Open access: articles freely available online
- High visibility within the field
- Retaining the copyright to your article

Submit your next manuscript at ► [springeropen.com](https://www.springeropen.com)